

RESEARCH ARTICLE

Solid-state characterization and dissolution properties of Fluvastatin sodium salt hydrates

AQ1 Silvia H.M. Borgmann¹, Larissa S. Bernardi¹, Gabriela S. Rauber¹, Paulo R. Oliveira¹, Carlos E.M. de Campos¹, Gustavo Monti², Silvia L. Cuffini¹, and Simone Cardoso¹

AQ2 ¹Federal University of Santa Catarina, Florianópolis, Brazil and ²Facultad de Matemática, Astronomía Y Física, Córdoba, Argentina

Abstract

The present study reports the solid-state properties of Fluvastatin sodium salt crystallized from different solvents for comparison with crystalline forms of the commercially available raw material and United States Pharmacopeia (USP) reference standard. FLV samples were characterized by several techniques; such as X-ray powder diffractometry, differential scanning calorimetry, thermogravimetry, liquid and solid-state nuclear magnetic resonance spectroscopy, diffuse reflectance infrared Fourier transform spectroscopy, and scanning electron microscopy. In addition, intrinsic dissolution rate (IDR) of samples was performed in order to study the influence of crystalline form and other factors on rate and extent of dissolution. Three different forms were found. The commercial raw material and Fluvastatin-ACN were identified as “form I” hydrate, the USP reference standard as “form II” hydrate and an ethanol solvate which presented a mixture of phases. Form I, with water content of 4%, was identified as monohydrate.

Keywords:

Introduction

Several drugs reduce low-density lipoprotein-cholesterol; fibrates, cholesterol absorption inhibitors, nicotinic acid and its derivatives, and statins. Statins are part of a remarkable class of cholesterol-lowering drugs. They are competitive inhibitors of 3-hydroxy-3-methyl-glutarylcoenzyme A (HMG-CoA) reductase, an enzyme that catalyzes a limiting step in cholesterol synthesis. Fluvastatin sodium (Figure 1) is the first inhibitor of HMG-CoA reductase of synthetic origin, structurally distinct from those statins produced by metabolism of fungi, such as lovastatin, pravastatin, and simvastatin. All HMG-CoA reductase inhibitors are hepatically metabolized; however, these drugs have subtle differences in their extent of hepatic absorption and excretion after oral administration.^[1–3] Fluvastatin sodium has a low systemic distribution, which helps to protect peripheral tissues of undesirable effects. In addition; the drug has a short-elimination half-life and extensive plasma protein binding.^[1,2]

Fluvastatin sodium was approved by the Food and Drug Administration (FDA) in 1998.^[4] The patent of Lescol was registered in 1994, and expired in 2011. Fluvastatin sodium is marketed as a racemic mixture of the two erythro enantiomers—(+) -3R,5S and (–) -3S, 5R—of which the 3R,5S form possesses >30 times the activity of the 3S,5R form.^[5–7]

Although the physical characterization of solid drugs has become an area of great interest in pharmacy, for some drugs, such as Fluvastatin sodium, studies of the characterization of the solid state and different crystalline forms have not been reported. Drug solid state characterization is an important step in pharmaceutical development due to its implications in physical and physicochemical factors (density, chemical stability, melting point, solubility, etc.) that may significantly affect the performance of drug products.^[8]

There are studies that have reported improvements in chemical and physical stability of Fluvastatin sodium through the interaction of drugs with polymers^[9] or by

Address for Correspondence: Dr. Simone Cardoso, Federal University of Santa Catarina, Florianópolis, 88040970 Brazil.

E-mail: simonegc@ccs.ufsc.br

(Received 11 May 2012; revised 04 August 2012; accepted 22 August 2012)

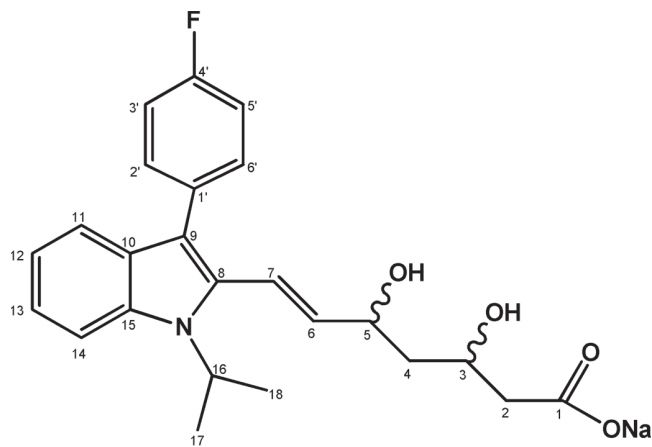


Figure 1. Chemical structure of Fluvastatin sodium (sodium (\pm) -(3R*,5S*,6E)-7-[3-(4-fluorophenyl)-1-isopropyl-1H-indol-2-yl]-3,5-dihydroxy-6-heptenoate; CAS n° 93957-55-2).

intercalating the drug in layered double hydroxide by using the coprecipitation method.^[10] However, the X-ray powder diffraction (XRPD) patterns reported in these studies have shown different crystalline structure for Fluvastatin sodium. Therefore, these results are valid only with those crystalline forms, and the performance of the final products could be different depending on the crystalline structure of Fluvastatin sodium used. It is noteworthy, that several patents related to crystalline forms of Fluvastatin sodium have been registered, but the solid-state characterization of the forms reported was incomplete, mainly related to dissolution properties.^[9-17] Fluvastatin sodium also exhibits hygroscopic nature, and it has been mentioned in some patents^[11-14,17] that small changes in the water content can cause deviations in the d values of characteristic peaks in the XRPD. In addition, crystalline hydrates of Fluvastatin sodium were prepared with water content ranges from 3 to 32%.^[12] United States Pharmacopeia (USP) monograph indicates a determination of water content before using the reference standard for the experiments, stating that FLV water content does not exceed 4%.^[18] Fluvastatin sodium raw material reports from the suppliers do not mention anything about the presence of hydrate forms, only the water content as it was mentioned before and at present, Fluvastatin sodium does not have the crystal structure determined.

The solubility and dissolution rate of active ingredients are of major importance in preformulation studies of pharmaceutical dosage forms. The intrinsic dissolution rate (IDR) has been used to characterize solid drugs and could be used to understand the relationship between the dissolution rate and the crystalline form.^[19] However, the effect of dissolution in different crystalline forms of Fluvastatin sodium has not been reported as yet. For all the reasons previously mentioned we chose/selected to study a solid-state characterization and the dissolution properties of different crystalline forms of Fluvastatin sodium from commercial samples (raw material and USP reference standard) and samples crystallized from different solvents, in order to contribute relevant information

about physicochemical properties for formulation design, performance improvement, and reproducibility quality of final products.

Materials and methods

Materials

The raw material of Fluvastatin sodium (Fluvastatin-RM) was obtained from a Chinese supplier, with a purity of 99.5%, declared in the certificate of analysis as sodium (\pm) -(3R*,5S*,6E)-7-[3-(4-fluorophenyl)-1-isopropyl-1H-indol-2-yl]-3,5-dihydroxy-6-heptenoate (CAS N° 93957-55-2). The reference substance of Fluvastatin sodium (Fluvastatin-USP; Lot: G0G313; purity 99.7%, CAS N° 93957-55-2) was purchased from the USP. Both samples, raw material and reference substance, were in racemic form. The raw material was presented as fine white powder, whereas Fluvastatin-USP was a yellow-color crystalline powder. All solvents used were of analytical reagent grade, and were used without further purification.

The crystallized samples were obtained by the method of crystallization by cooling. The procedure was carried out using various solvents. The solvents used were class 2 (acetonitrile and methanol) and class 3 (ethanol),^[20] widely used in the final stages of crystallization, and as a co-solvent, in different proportions and in two temperatures (8°C and 25°C). Only in acetonitrile and ethanol did the samples present adequate crystallization. A predetermined mass of Fluvastatin-RM, to reach the saturation condition of the solution at room temperature, was dissolved in solvent at $40 \pm 0.5^\circ\text{C}$, and was constantly stirred until complete solubilization. After solubilization, the samples were cooled to 8°C in a refrigerator and 25°C, long enough to crystallize. By changing the temperature of the solution, a condition of supersaturation was reached. The crystals obtained from the different conditions were stored in a refrigerator. The samples crystallized in acetonitrile and ethanol were chosen to continue the study as they were the ones that presented different crystalline structures by XRD and reproducibility in crystallization. They were named Fluvastatin-ACN and Fluvastatin-EOH, respectively.

Solid-state characterization techniques and experimental methods

XRPD

X-ray diffraction patterns were obtained using an θ - θ Xpert Pro Multi-Purpose Diffractometer PANalytical (Eindhoven, the Netherlands) with Cu K α tube ($\lambda = 1.5418 \text{ \AA}$) and Ni filter, 45 kV voltage and a current of 40 mA in the range of 5–60 (2θ), 0.016 (step) and 30 s equipped with X'Celerator detector. The divergent and anti-scattering slits were 0.5° and 0.25°, respectively.

Scanning electronic microscopy (SEM)

The photomicrographs were taken in a Scanning Electron Microscope Philips XL30 model (Eindhoven, the Netherlands). The samples were placed on metal stubs

using double-sided tape, and were vacuum-coated with gold (350 Å) in Polaron E 5000 sputter coating unit. The samples were analyzed directly by scanning electronic microscopy (SEM).

Thermal analysis: DSC and TG

The differential scanning calorimetry (DSC) curves were obtained using a Shimadzu DSC-60 (Kyoto, Japan) cell in a dynamic atmosphere of nitrogen with a flow of 50 mL/min. Approximately 2 mg of each sample were weighed and placed in sealed aluminum crucibles. Analyses were performed in the range 40–300°C with a heating rate of 10°C/min. The DSC cell was calibrated with indium (melting point of 156.6°C and enthalpy of fusion of 28.54 J/g) and zinc (melting point of 419.6°C). The thermogravimetry (TG)/DTG measurements were carried out in Shimadzu TGA-50 (Kyoto, Japan) under a dynamic thermal balance atmosphere of nitrogen with a flow of 50 mL/min. Approximately 6 mg of each sample were weighed and placed in platinum crucibles. Analyses were performed in the range 40 to 300°C with a heating rate of 10°C/min. The equipment was previously calibrated with standard calcium oxalate.

FTIR and Raman spectroscopy

The Fourier-transform infra-red (FTIR) spectra were measured on a Shimadzu IR Prestige spectrophotometer—(Kyoto, Japan), with a scan range of 4000–600 cm⁻¹, with spectral resolution of 4 cm⁻¹ and averaged over 32 scans. A spectrum of the background was obtained for each experimental condition.

The Raman experiments were carried out in a PeakSeeker 785 (RAM - PRO - 785) Raman system operating with a diode laser of 785 nm and 300 mW at the source. The collected Raman radiation was dispersed with a grating and focused on a Peltier-cooled charge-coupled device allowing a spectral resolution of 6 cm⁻¹ to be obtained. The laser was focused on the sample by the ×4 objective lens of a microscope giving a spot of ~2-µm diameter. All spectra were recorded in the spectral window of 200–1800 cm⁻¹ with the same acquisition time (30 s). The sample powders were analyzed in glass slides at room temperature.

Solid-state nuclear magnetic resonance (ssNMR)

High resolution ¹³C solid-state spectra for the APIs were recorded using the ramp CP/MAS sequence with proton decoupling during acquisition. All the solid state NMR experiments were performed at room temperature in a Bruker Avance II spectrometer (Bruker, Karlsruhe, Germany) operating at 300.13 MHz for protons and equipped with a 4 mm MAS probe. The operating frequency for carbons was 75.46 MHz. Adamantane was used as an external reference for the ¹³C spectra and to set the Hartmann-Hahn matching condition in the cross polarization experiments. Spinning rate was 10 kHz. The number of transients for each compound was 2048 in order to obtain an adequate signal to noise ratio. The

recycling time was 5 s and the contact time during CP was 2.5 ms for all the samples. SPINAL 64 sequence was used for decoupling during acquisition with a proton field H_{1H} satisfying ω_{1H}/2π = γ_H H_{1H}/2π = 78.2 kHz. Quaternary carbon edition spectra were recorded for all the samples. These spectra were acquired with the non-quaternary suppression (NQS) sequence, where the ¹H and ¹³C radio-frequency (rf) fields are removed during 40 µs after CP and before the acquisition. This delay allows the carbon magnetization to decay because of the ¹H-¹³C dipolar coupling, resulting in spectra where CH and CH₂ are substantially removed. This experiment allows us, then, to identify quaternary carbon signals and methyl groups.

Determination of water by Karl-Fischer (KF)

The water content in the samples was measured by KF method using titrator Mettler DL 38 (Mettler, Greifensee, Switzerland). Ultra-pure water (Milli-Q) was used to standardize the KF reagent and spectroscopic grade methanol for titration of the samples. The water content of all samples was expressed as percentage (wt/wt %).

IDR

The IDR was determined using the USP apparatus for intrinsic dissolution through the pressure plate method. One tablet of ~13 mm diameter was obtained by compressing (400 kgf for a period of 1 min) 100 mg of powdered sample using a hydraulic press. Studies were carried out to determine whether compression of the drug into IDR disks led to any change in crystalline form. XRPD analyses showed that compression of the sample powder did not modify the crystalline form of the drug. Dissolution studies were performed in duplicate in a Varian dissolution test system VK 7000 (Varian, NJ, USA) using 900 ml of phosphate buffer pH 6.8 at 37 ± 0.5°C. The exposed surface of 0.5 cm² of the compacted sample was positioned 2.5 cm from the bottom of the vessel. As described in USP^[18] the rod immediately began stirring at 100 rpm. Aliquots of 5 mL were withdrawn at predetermined times (5, 10, 15, 30, 45, 60, 75, 90, 105, and 120 min). Equal amounts of fresh dissolution medium were replaced immediately after every sampling. Quantification was carried out using the liquid chromatography method previously developed and validated.^[21] Analyses were performed in Xbridge Waters column C18 (12.5 cm × 3.9 mm, 4 mM) at room temperature using Shimadzu LC-10A chromatograph (Shimadzu, Kyoto, Japan) equipped with a pump LC-10AD, degasser DGU-14A, variable wavelength detector SPD-10AV (set at 238 nm) and system controller unit SCL-10AVP. The mobile phase consisted of methanol and water (70:30, vol/vol) with pH adjusted to 3.0 with phosphoric acid at a flow rate of 1 mL/min. The IDR was calculated from the slope, based on the release of the drug into the dissolution medium.^[18,19,21] Only the values above of quantitation limit of the method (2.0 µg/ml) were taken into account.

Results

Solid-state characterization of samples

Fluvastatin sodium is a class I drug^[22-25] with hygroscopic nature. According to USP, the water content of Fluvastatin-USP must be determined before using it in experiments, and should not be >4%.^[18] The result obtained in this work with Fluvastatin-USP was 9.2%. Fluvastatin-RM was acquired containing 4.1% water, according to a report issued by the supplier. It is worth highlighting that in the reports of Fluvastatin-RM and Fluvastatin-USP, Fluvastatin was not mentioned as a hydrated drug.

The results of the XRPD of the samples are shown in Figure 2. Fluvastatin-ACN presented a well-defined pattern of reflections, proving that the sample was crystalline. Fluvastatin-RM showed the same positions of pattern reflections as the Fluvastatin-ACN, with subtle differences in intensity. This could be attributed to the effect of preferential orientation, which would explain the difference of intensity in the patterns. Therefore, these results confirmed that the Fluvastatin-ACN and Fluvastatin-RM correspond to the same crystalline structure. The diffraction pattern of Fluvastatin-USP (Figure 2C) presented a crystalline structure with a higher level of disorder in the lattice, and with differences in the reflection positions when compared to the previous crystalline forms analyzed. Therefore, Fluvastatin-USP was identified as another crystalline form or polymorph of Fluvastatin sodium.

In the case of Fluvastatin-EOH, many reflections with a significant expansion and a high superposition were observed (Figure 2D). These characteristics of X-ray diffraction patterns, in general, make it difficult to identify the phases. The low crystallinity of this sample and a high level of disorder were evident. Due to these characteristics it was not clear, from the XRPD pattern analysis, if the Fluvastatin-EOH corresponded to a new pure crystalline form, different from those previously mentioned (Fluvastatin-RM/Fluvastatin-ACN and Fluvastatin-USP), or a mixture of crystalline forms. Therefore, it was very important to complement the solid state characterization of the crystalline forms, using other techniques.

To characterize the morphology of the samples, scanning electron microscopy was used and the micrographs are shown in Figure 3. The Fluvastatin-ACN particles presented acicular habits and a well-defined geometry which indicates good crystallinity in the sample. The morphology of Fluvastatin-RM presented a different aspect in relation to the previous habit and a geometry of the particles which was not very well-defined. The size of the particles, qualitatively observed by SEM, was lower than that shown in Fluvastatin-ACN. The Fluvastatin-EOH and Fluvastatin-USP samples presented larger sized particles, with irregular shapes, evidencing a higher degree of disorder; especially the FLV-EOH sample, which presented a typical aspect of samples with a high degree of disorder.

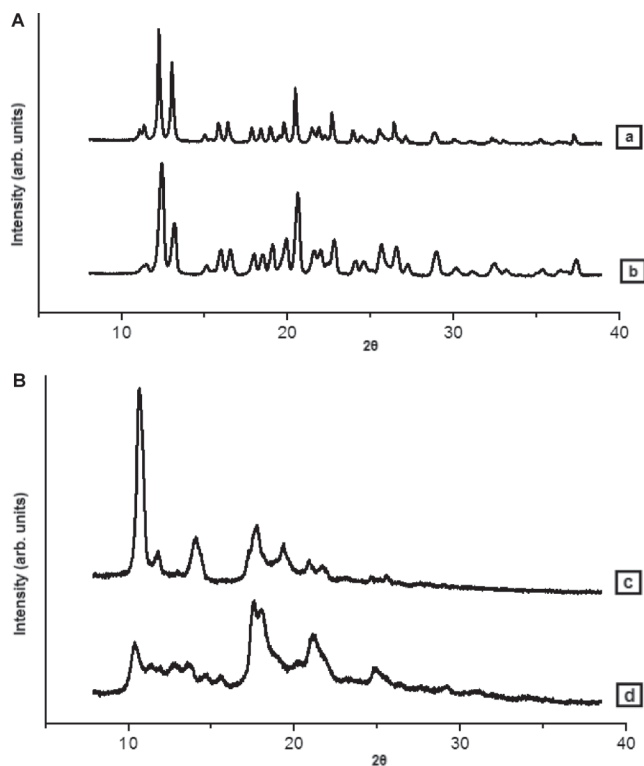


Figure 2. X-ray patterns of the different crystalline forms of Fluvastatin sodium. (A) Fluvastatin-ACN; (B) Fluvastatin-USP; (C) Fluvastatin-EOH; (D) Fluvastatin-RM.

The study of thermal properties of the different solid forms provided very important results, such as: water loss behavior and strength of interaction between water and the drug molecule. DSC curves of samples are shown in Figure 4. The samples presented two endothermic events, but only the event close to 145°C was the same in the four samples. The Fluvastatin-ACN and Fluvastatin-RM samples presented the same profiles, especially at temperatures of endotherms (Table 1), whereas the Fluvastatin-USP showed an endotherm at around 107.21°C, and the other at 149.34°C. In the case of Fluvastatin-EOH curve, the first endothermic event appeared at 120.20°C and the second event at 149.34. This data clearly showed the differences between Fluvastatin-RM and Fluvastatin-USP and the similarities in comparison to Fluvastatin-RM and Fluvastatin-ACN which are in agreement with the results obtained by XRPD. However, to have a deeper knowledge of these samples, it was necessary to study the mass loss compared to the endothermic processes observed, by using TG and KF.

A high percentage of water was observed in all samples studied. The weight loss values obtained by TG for FLV-USP and FLV-EOH were unreliable in comparison with those obtained by KF. This behavior can be attributed to the variation in the initial water loss detected in the case of FLV-USP and FLV-EOH. This value was out of control due to the impact of the flow of nitrogen during the weight stabilization in these samples. There could be a

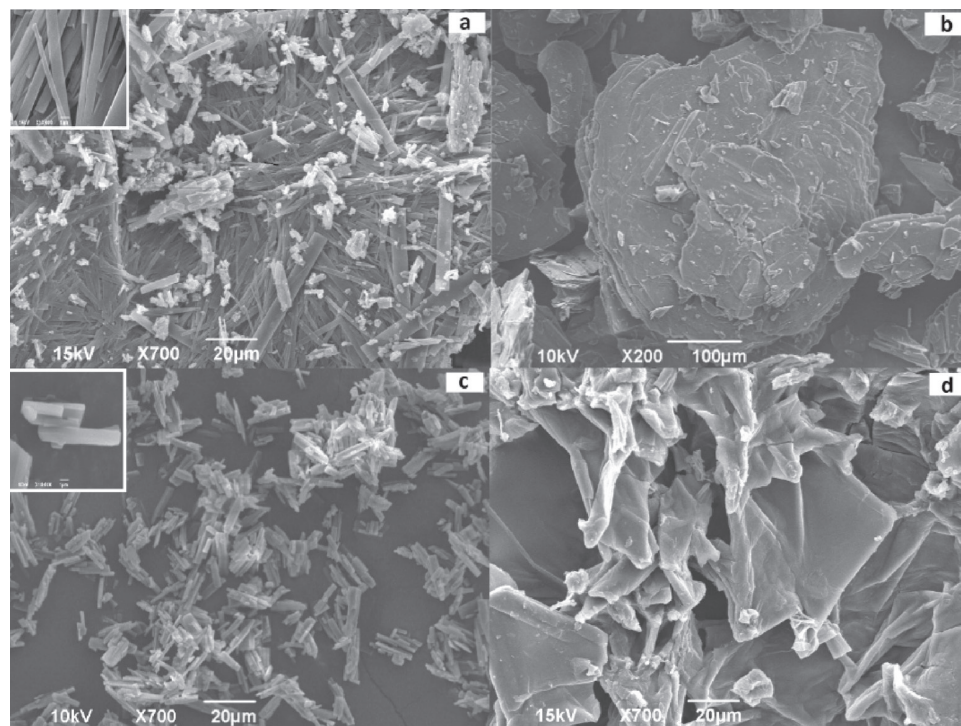


Figure 3. Scanning electron microscopy of the different forms of Fluvastatin sodium. (A) Fluvastatin-ACN; (B) Fluvastatin-USP; (C) Fluvastatin-RM; (D) Fluvastatin-EOH.

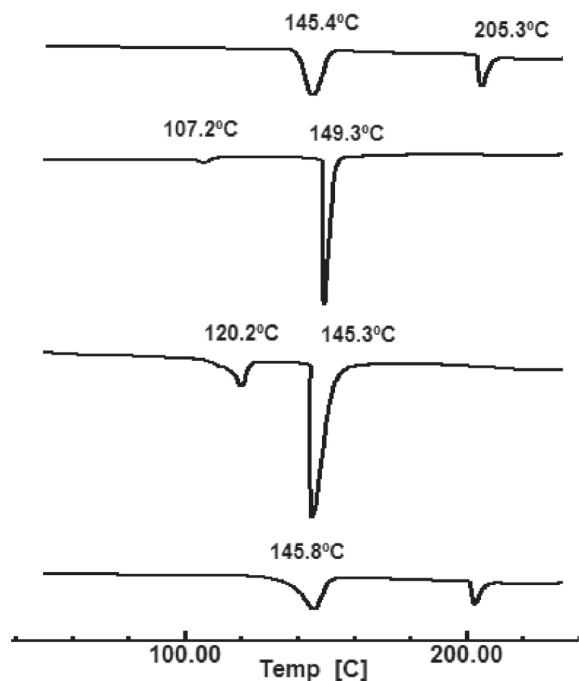


Figure 4. Differential scanning calorimetry (DSC) curves of different crystalline forms of Fluvastatin sodium. (A) Fluvastatin-ACN; (B) Fluvastatin-USP; (C) Fluvastatin-EOH; (D) Fluvastatin-RM.

reason for the variation in the values of mass loss and the difference found between the values obtained by TG and KF. However, in the case of FLV-ACN and FLV-RM, the values of mass loss by TG were in acceptable agreement to those observed by KF. Water content ~4% determined for FLV-RM might correspond to a monohydrate drug.

Table 1. Results obtained with DSC curves of the different crystalline forms of Fluvastatin sodium.

| Samples | Temperature peak (°C) | ΔH fusion (J/g) | Temperature peak (°C) | ΔH fusion (J/g) |
|---------|-----------------------|-------------------------|-----------------------|-------------------------|
| FLV-ACN | 145.40 | 106.34 | 205.27 | 137.29 |
| FLV-EOH | 120.20 | 46.40 | 145.31 | 245.69 |
| FLV-USP | 107.21 | 14.03 | 149.34 | 137.29 |
| FLV-RM | 145.82 | 111.04 | 202.81 | 26.69 |

DSC, differential scanning calorimetry.

In order to determine whether Fluvastatin-EOH was a solvate, incorporating ethanol into its structure, we conducted studies through different spectroscopic techniques. The techniques used were: NMR, FT-IR, and Raman spectroscopies. The study by NMR spectroscopy was performed both in solution (DMSO) and as a solid. Thus, it was possible to obtain complete information on the molecular and crystalline structure of Fluvastatin sodium and also crystal structural evidence, such as: number of molecules present in the asymmetric unit and the presence or absence of solvent incorporated in the crystalline structure.

The NMR spectrum of the Fluvastatin sodium in DMSO showed the chemical shifts detailed in Table 3 (the carbon numbering is shown in Figure 1). The values of the displacements found through the experiments are in agreement with the shifts already reported in literature,^[26] but some differences can be observed related to the use of other solvents which are inherent to this process.^[27] According to Cermola et al.^[26] the chemical shifts in 113.3 ppm was attributed the value of C14. However, we believe that this value may be a typing error, since it

does not make sense that C9 and C14 present the same displacements.

The ^{13}C CP-MAS spectra of Fluvastatin-RM and Fluvastatin-EOH are shown in Figure 5. Table 3 reports the ^{13}C chemical shifts for these samples. The NQS spectra for Fluvastatin-RM and Fluvastatin-EOH are illustrated in Figure 6. The atomic labels correspond to Figure 1.

The carbons of Fluvastatin-RM spectra were selected; taking into account the NQS data of the compound (see Figure 6). Furthermore, a reference Cermola et al.^[26] was used to obtain ^{13}C - ^{19}F scalar spin-spin coupling information, ^{13}C - ^{14}N residual dipolar coupling and chemical shift calculations.

The ^{13}C spectrum of Fluvastatin-RM indicated that there was only one molecule per asymmetric unit. We were able to observe the splitting of C 4' signal, 158.1 and 162.5 ppm, due to the scalar spin-spin coupling to ^{19}F nucleus. The ^{13}C , ^{19}F scalar spin-spin coupling constant was (267 ± 5) Hz, and was in good agreement with that obtained from solution spectrum (242.8 ± 0.4) Hz, and close to those reported in some fluorinated steroids.^[28,29] The C16 resonance showed the characteristic broadening due to coupling to ^{14}N quadrupolar nucleus. This was also clearly observed for C15 and C8 on the NQS spectrum.

The ^{13}C spectrum of Fluvastatin-EOH showed many differences with the Fluvastatin-RM one. The resonance of methyl carbons, a single peak in the Fluvastatin-RM spectrum, showed two lines with 2:1 intensity ratio. This fact suggested the presence of at least two molecules in the asymmetric unit or a mixture of crystalline phases. In the region 100–150 ppm, the Fluvastatin-EOH ^{13}C spectrum showed two additional resonances compared with the Fluvastatin-RM ^{13}C spectrum, at 139.0 and 120.8 ppm. The other resonances were coincident in the two spectra. In the region 40–80 ppm, the Fluvastatin-EOH ^{13}C spectrum showed four additional resonances compared with the Fluvastatin-EOH ^{13}C spectrum, at 45.3, 68.5, and 70.9 and 72.3 ppm. The signals at 45.3 and 68.5 were not suppressed by the NQS pulse sequence (see Figure 6). The NQS spectra of Fluvastatin-RM and Fluvastatin-EOH were very similar, except for the presence of the resonances at 45.3 and 68.5 ppm in the Fluvastatin-EOH NQS spectrum. These facts strongly indicated that the resonance corresponded to CH_3 groups of solvent molecules in different environments in the crystal structure.^[29]

The FTIR spectra of the samples are shown in Figure 7. The interpretation of the infrared spectra was

Table 2. Results obtained with TG curves and water determination by Karl-Fischer (KF) of the different crystalline forms of Fluvastatin sodium.

| Sample | FLV-ACN | | FLV-RM | |
|--------|-------------|------|-------------|------|
| | Range (°C) | % | Range (°C) | % |
| | 34.3–43.3 | 0.04 | 31.9–44.9 | 0.4 |
| | 108.2–125.6 | 2.9 | 109.2–126.5 | 3.6 |
| | | | 240.6–281.9 | 21.3 |
| KF | 4.95% | | 3.93% | |

TG, thermogravimetry.

based on the presence of the most important functional groups. The subtle differences found between the spectra of the crystalline forms of Fluvastatin sodium may indicate structural changes and provide information on intermolecular interactions of the samples. The main differences were found in the region between 1557 and 1587 cm^{-1} , a region which is indicative of salt as carboxylate. Note that for the two samples that were identified by XRPD and DSC as the same crystalline form, Fluvastatin-ACN and Fluvastatin-RM, presented a frequency value of 1587 cm^{-1} and 1585 cm^{-1} , respectively. However, the sample Fluvastatin-USP showed a value of 1568 cm^{-1} . There are different values described in literature for the same carboxylate group of sodium Fluvastatin in 1576 cm^{-1} ^[9] and 1573 cm^{-1} .^[10] It is important to highlight that the XRPD patterns presented in previously published work^[9,10] show significant differences between them, making it evident that they are different crystalline structures. Therefore, the difference found in the FTIR spectra bands in comparison with our results could be explained by the fact that they are different crystalline forms.

The bands, in the region between 3300 and 3500 cm^{-1} showed, in all samples, the frequency modes of the stretching of the functional group hydroxide (OH) corresponding to the presence of water in the region between 1500 and 800 cm^{-1} . Similarities found between Fluvastatin-RM and Fluvastatin-ACN can be observed in the spectra,

Table 3. Spectral data of ^{13}C NMR FLV in DMSO, data reported in CD_3OD comparative to ^{13}C CP/MAS NMR solid.

| Carbon No. | ^{13}C NMR (CD3OD) | ^{13}C NMR (DMSO) | Solid |
|------------|-----------------------------|----------------------------|-------------------|
| 1 | 180.2 | 176.9 | 181.3 |
| 2 | 45.3 ^a | 45.07 ^a | 42.5 ^a |
| 3 | 68.8 | 66.26 | 65.2 |
| 4 | 45.6 ^a | 44.03 ^a | 44.0 ^a |
| 5 | 72.2 | 69.25 | 70.3 |
| 6 | 141.4 | 142.2 | 136.9 |
| 7 | 123.1 | 117.13 | 118.4 |
| 8 | 130.2 | 134.68 | 133.0 |
| 9 | 113.3 | 113.24 | 114.8 |
| 10 | 130.2 | 127.99 | 127.6 |
| 11 | 120.6 | 119.02 | 121.4 |
| 12 | 120.6 | 119.02 | 121.4 |
| 13 | 121.0 | 119.93 | 121.4 |
| 14 | 113.3 | 121.88 | 122.0 |
| 15 | 138.0 | 135.08 | 135.8 |
| 16 | 48.9 | 47.54 | 48.0 |
| 17 | 22.4 | 21.76 | 19.9 |
| 18 | 22.4 | 21.76 | 19.9 |
| 1' | 134.6 | 131.95 | 131.3 |
| 2' | 133.7 | 132.11 | 131.9 |
| 3' | 116.7 | 115.7 | 112.7 |
| 4' | 163.5 | 161.02 | 160.8 |
| 5' | 116.7 | 115.7 | 112.7 |
| 6' | 133.7 | 132.11 | 131.9 |

^aThe value of carbon 2 and 4 may be interchanged.

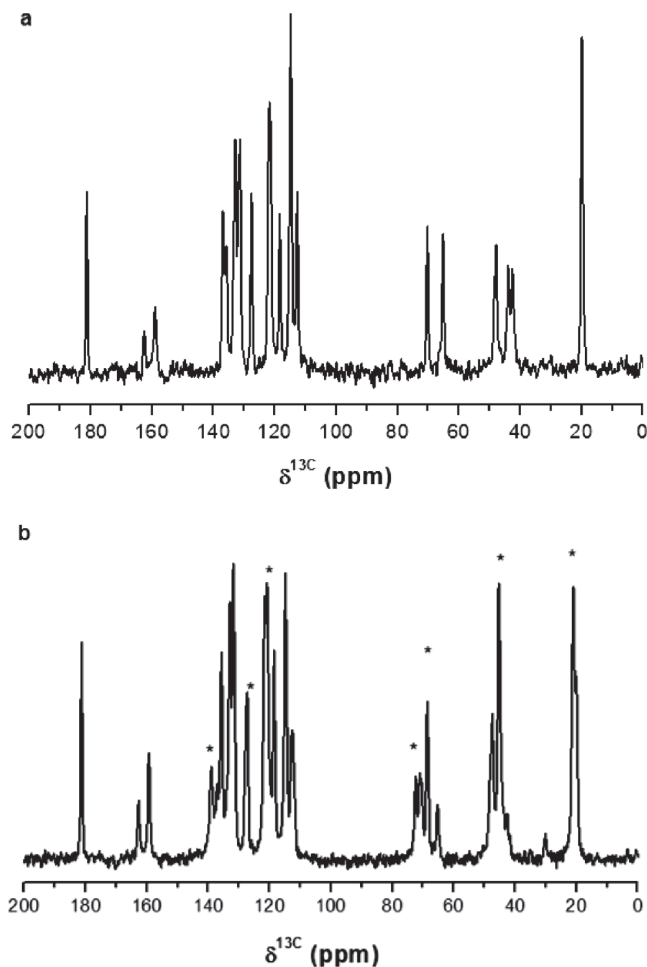


Figure 5. Spectra ^{13}C CP/MAS NMR solid of (A) Fluvastatin-RM and (B) Fluvastatin-EOH (*different chemical shifts of those found in Fluvastatin-RM).

and these differences are related to Fluvastatin-USP and Fluvastatin-EOH. The amino group can be identified by the band found in the region of 1215 cm^{-1} , whereas the halogen fluorine present in the molecule can be identified by the band presented around 1048 cm^{-1} .

The Raman spectra collected for Fluvastatin-RM and Fluvastatin-EOH are shown in Figure 8. The Raman spectrum of Fluvastatin-RM showed a predominance of a well-defined set of signals. The Raman spectrum found in the literature^[9] is not clearly defined for correct comparison with the data in Figure 8. The sample of Fluvastatin-EOH presented the same sequence of signals as the FLV-RM, but in the latter sample there was a halo in the background, indicating a disorder in the crystalline lattice.

IDR

As mentioned earlier, the characterization and understanding of the solid state of polymorphs and solvates of a particular drug provide relevant information for both quality control and for product innovation or development. Thus, an important property to be analyzed is the IDR, which may be correlated to the properties previously

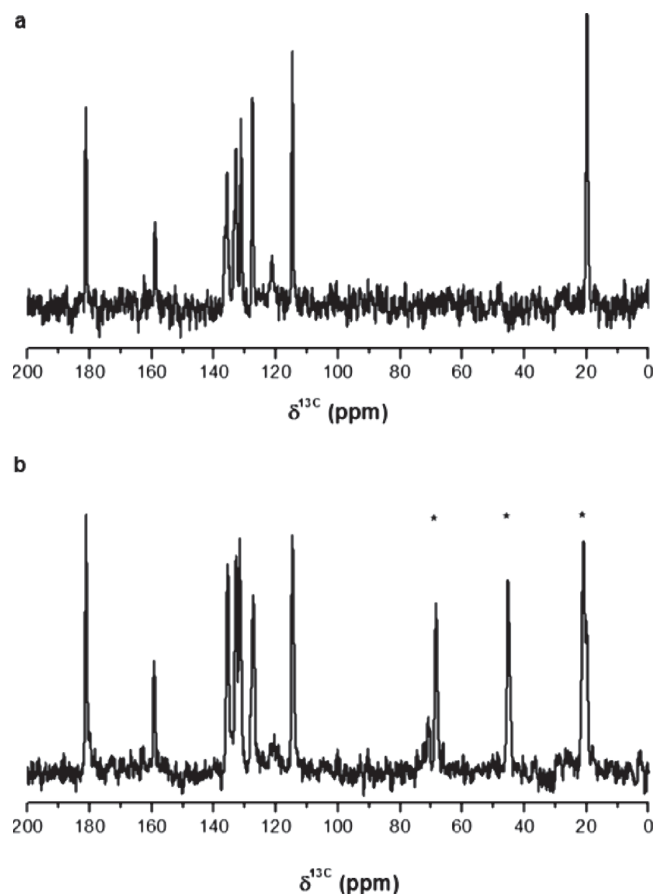


Figure 6. Spectra ^{13}C CP/MAS NMR solid NQS of (A) Fluvastatin-RM and (B) Fluvastatin-EOH (*different chemical shifts of those found in Fluvastatin-RM).

studied with their impact on a biopharmaceutical level. The IDR values can be modified by polymorphic forms or crystalline structure, morphology, or crystalline habit, crystalline size, a mixture of phases and degree of order/disorder of materials. Knowing the behavior of the IDR of the samples is possible to determine which of the solid state properties have the most impact in the performance of the drug.

The samples analyzed with IDR were Fluvastatin-RM and Fluvastatin-ACN (Figure 9), since we did not have enough quantity of mass for the others, Fluvastatin-USP and Fluvastatin-EOH. The results of IDR are shown from 30 min because the values were above the detection limit of HPLC method. In the IDR experiments, linearity was verified in all samples and the values of IDR are detailed in Table 4.

Discussion

The results of the XRPD and FTIR spectroscopy showed that Fluvastatin sodium presents two crystalline forms corresponding to Fluvastatin-ACN and Fluvastatin-USP. With the ethanol crystallization (Fluvastatin-EOH) a mixture of phases was determined also using Raman and CP/MAS ^{13}C NMR spectroscopies. The crystalline form

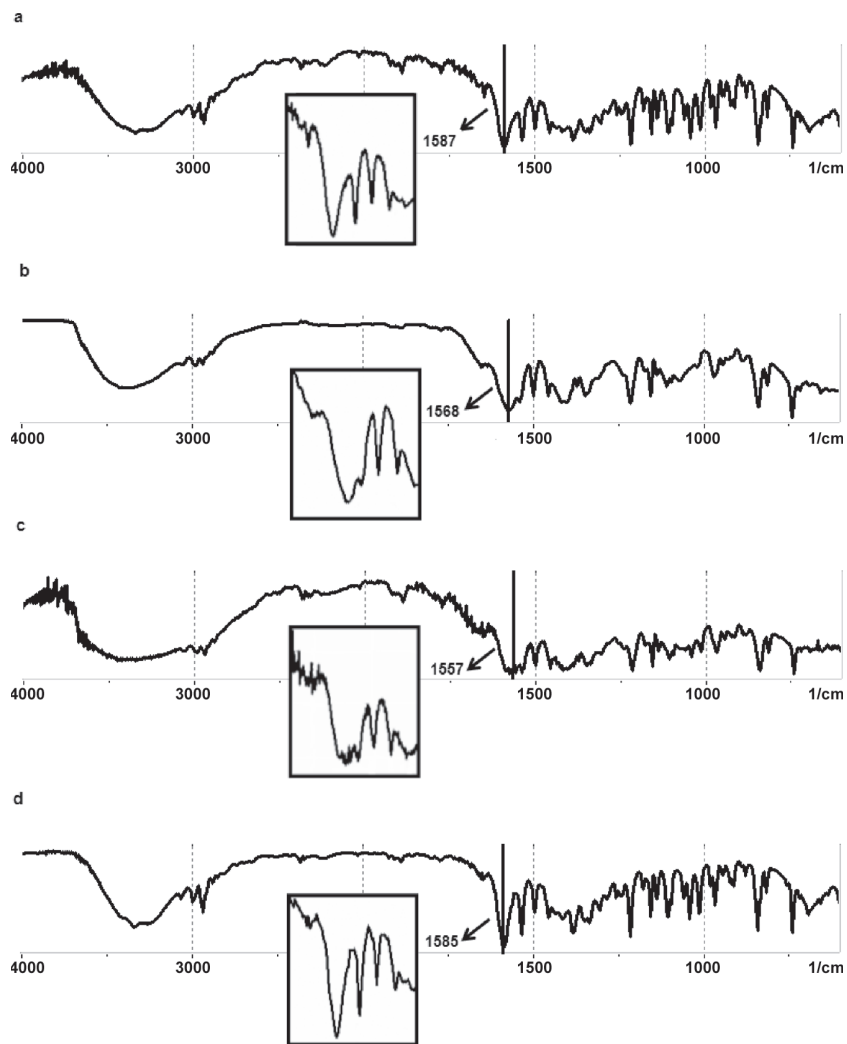


Figure 7. Infra-red spectra obtained from the different crystalline forms of Fluvastatin sodium. (A) Fluvastatin-ACN; (B) Fluvastatin-USP; (C) Fluvastatin-EOH; (D) Fluvastatin-RM.

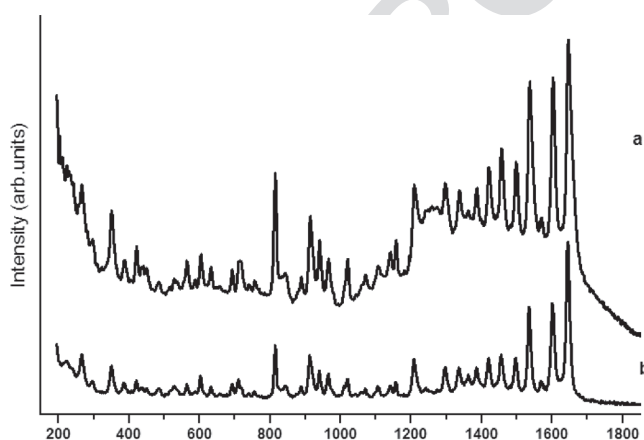


Figure 8. Raman spectrum obtained from the crystals (A) Fluvastatin-ACN (B) Fluvastatin-EOH ($1800-200\text{ cm}^{-1}$).

of Fluvastatin-RM was coincident with the Fluvastatin-ACN sample.

After the comparison of XRPD patterns of Fluvastatin sodium of several patents^[8-10] and the patterns reported

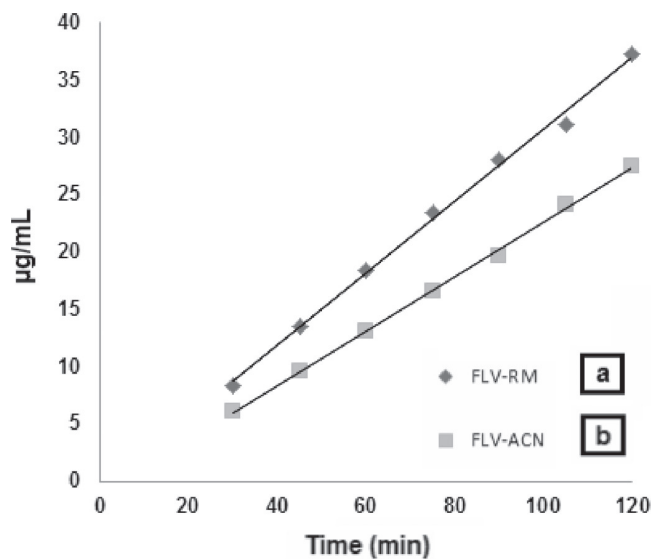


Figure 9. Graphic representation of IDR of the different crystalline forms of Fluvastatin sodium. (A) Fluvastatin-RM (FLV-RM); (B) Fluvastatin-ACN (FLV-ACN).

Table 4. Equation of the line and r obtained with the graphical representation of the results of intrinsic dissolution testing of Fluvastatin sodium and calculated values of the IDR.

| Sample | Equation of the line | r | IDR (mg/min/ cm ²) \pm SD |
|---------|------------------------|--------|--|
| FLV-RM | $y = 0.3132x - 0.6294$ | 0.9984 | 0.166 ± 0.004 |
| FLV-ACN | $y = 0.238x - 1.1832$ | 0.9994 | 0.095 ± 0.002 |

IDR, intrinsic dissolution rate.

in our work, we concluded that Fluvastatin-RM and Fluvastatin-ACN correspond to racemic crystalline form designated as form A monohydrate reported in patent US 6124340.^[11] In addition, Fluvastatin-USP could be identified as crystalline form designated as form A (racemic mixture) in patent US 6858643 B2.^[13] However, the form D reported in patent US 003266 A1,^[12] prepared under humid conditions, exhibits peaks in the XRPD pattern which are also in agreement with the Fluvastatin-USP pattern. Due to the ambiguity of the nomenclature used in these patents, we decided to designate the polymorph of Fluvastatin-RM and Fluvastatin-ACN as form 1 and the polymorph for Fluvastatin-USP as form 2.

Despite a rigorous monitoring and control of the stock conditions, in the case of a drug that has a strong tendency toward the incorporation of water, the water content could be a challenge, especially in places where the relative humidity ranges from 60% to 80%.^[30] All the forms of Fluvastatin sodium studied in this work were identified as hydrates. The affinity of hydration of Fluvastatin sodium can be analyzed also taking into account the chemical groups present in the molecules.^[31] The compound Fluvastatin sodium contains a sodium ion, a carboxylate group, two hydroxyl groups and one fluorine atom. Each of these groups has an affinity for moisture, respectively, 51.8, 34.7, 12.7, and 3.5%. Thus, this molecule has a large capacity and/or a tendency to include water in their crystal structure. If we look at the current Cambridge Crystallographic Data Base (CSD) (with restrictions: only organic, no powder, $R < 10\%$), compounds containing a carboxylate group with a sodium ion are 189 entries and 130 of them contain water molecules. Therefore, these types of compounds have at least a 69% chance of including water in its crystal structure. Finally, solid-state characterization results and the affinity analysis are in agreement with Fluvastatin solid form 1 identified as monohydrates and form 2 as hydrate with variable water content. Fluvastatin-EOH was a mixture of solid forms, one phase more disordered or with disordered solvent (ethanol/water) in the lattice. Fluvastatin-EOH showed that the solvent was incorporated into its structure. This disorder could be due to very high water content, $>16\%$, but also by the presence of solvent (ethanol). Therefore, another phase of the mixture could be a solvate with ethanol and water. Finally, the values of the IDR to Fluvastatin-RM relative to Fluvastatin-ACN were statistically different ($\alpha = 0.05$, $p < 0.1$). IDR eliminates the effect of particle size distribution;^[18] therefore, it

may not be considered a determining factor. However, results which demonstrate that the crystalline habit can change the speed of dissolution have been reported.^[32] Therefore, in the case of Fluvastatin sodium, IDR might be modified not only by the crystalline structure, but also by other characteristics of the solid form such as morphology. Both samples, Fluvastatin-RM and Fluvastatin-ACN, presented the same crystalline structure; hence the difference in the IDR might be caused by the crystalline habits.

Conclusion

The study of solid-state properties of the samples Fluvastatin-RM, Fluvastatin-USP, and Fluvastatin-ACN showed that they are hydrates with different crystalline forms. The samples Fluvastatin-RM and Fluvastatin-ACN were identified as form I being different from the Fluvastatin-USP which is designated as form II. However, Fluvastatin-EOH is a solvate with a mixture of phases.

Form I presented a good crystallinity evidenced by the XRPD patterns and morphology by SEM, and had a single Fluvastatin sodium molecule in the asymmetric unit. Form I was identified as monohydrate with 4% of water content. Fluvastatin-RM and Fluvastatin-ACN presented the same crystalline structure (form I) but different morphology and also different behaviors in IDR. Fluvastatin-RM presented a higher dissolution rate, showing that not only polymorphism, but also the morphology of the raw materials could modify the intrinsic dissolution. Another two crystalline forms were analyzed: Form II hydrate, corresponding to USP reference standard, identified after the stabilization of water content around 9% and Fluvastatin-EOH solvate which presented a mixture of phases (form I and other phase with a high disorder in the crystal lattice).

Declaration of interest

The authors report no declarations of interest.

References

- Levy RI, Troendle AJ, Fattu JM. A quarter century of drug treatment of dyslipoproteinemia, with a focus on the new HMG-CoA reductase inhibitor fluvastatin. *Circulation* 1993;87:III45-III53.
- Blum CB. Comparison of properties of four inhibitors of 3-hydroxy-3-methylglutaryl-coenzyme A reductase. *Am J Cardiol* 1994;73:3D-11D.
- Othawa M, Uchiyama N, Saito Y, Suzuki A, Tanno C. Phase I study of MK-733, an inhibitor of HMG-CoA reductase II, Pharmacokinetics of MK-733 in healthy subjects after single and multiple oral administration. *Rinsho Yakaku* 1989;5:1123-1140.
- Food and Drug Administration. <<http://www.fda.gov/CDER/>>. Accessed on 22 August 2011.
- Trung TQ, Dung PT, Hoan NN, Kim DJ, Lee JH, Kim KH. Chiral separation of fluvastatin enantiomers by capillary electrophoresis. *Arch Pharm Res* 2008;31:1066-1072.
- Lijj (2009). Triumph of the heart: the story of statins. 88.

7. Zacharia JT, Tanaka T, Hayashi M. Facile and highly enantioselective synthesis of (+)- and (-)-Fluvastatin and their analogues 2010;75:7514–7518.
8. Sorrentia M, Catenaccia L, Brunib G, Luppig B, Biguccic F, Bettinetti G. Solid-state characterization of tacrine hydrochloride. *J Pharm Biom Anal* 2012; 63:53–61.
9. Papageorgiou GZ, Papadimitriou S, Karavas E, Georganakis E, Docoslis A, Bikiaris D. Improvement in chemical and physical stability of fluvastatin drug through hydrogen bonding interactions with different polymer matrices. *Curr Drug Deliv* 2009;6:101–112.
10. Panda HS, Srivastava R, Bahadur D. In-vitro release kinetics and stability of anticardiovascular drugs-intercalated layered double hydroxide nanohybrids. *J Phys Chem B* 2009;113:15090–15100.
11. Horwath K. Polymorphic compounds. 2000. Patent application number: US 6124340. <<http://ip.com/patent/US6124340>>. Accessed on 22 August 2011.
12. Van der Schaaf PA, Marcolli C, Szelagiewicz M, Burkhard A, Wolleb H, Wolleb A. Crystalline forms. Patent application number: US 0032666A1. <<http://ip.com/patapp/US20030032666>>. Accessed on 22 August 2011.
13. Van Der Schaaf PA, Wolleb H, Wolleb A, Marcolli C, Szelagiewicz M, Burkhard A, Freiermuth B. Crystalline forms of fluvastatin sodium. Patent application number: US 6858643B2, 2005. <<http://ip.com/patent/US6858643>>. Accessed on 22 August 2011.
14. Van Der Schaaf PA, Blatter F, Szelagiewicz M. Crystalline form of fluvastatin sodium. 2006. Patent application number: US 02041167A1. <<http://ip.com/patapp/US20060241167>>. Accessed on 22 August 2011.
15. Huang L. Anhydrous amorphous form of fluvastatin. Patent application number: US 7241800, 2007. <<http://www.patentgenius.com/patent/7241800.html>>. Accessed on 22 August 2011.
16. Chavhan B, Awasthi AK, Aggarwal R, Beena RS, Paul S, Thaper RK, Dubey SK. Novel polymorphic forms of fluvastatin sodium and process for preparing the same. 2008. Patent application number: 20080207919. <<http://www.faqs.org/patents/app/20080207919>>. Accessed on 22 August 2011.
17. Lifshitz-Liron HR, Koltai NT, Aronhime RJ, Perlman KSN, Avhar-Maydan GS. Fluvastatin crystal forms, processes for preparing them, compositions containing them and methods to using them. 2009. Patent application number: US 0209611A1. <<http://ip.com/patapp/US20090209611>>. Accessed on 22 August 2011.
18. USP 34, The United States Pharmacopeia. Rockville, MD: United States Pharmacopoeia Convention Inc. 2011.
19. Zakeri-Milani P, Barzegar-Jalali M, Azimi M, Valizadeh H. Biopharmaceutical classification of drugs using intrinsic dissolution rate (IDR) and rat intestinal permeability. *Eur J Pharm Biopharm* 2009;73:102–106.
20. Mirmehrabi M, Rohani S. An approach to solvent screening for crystallization of polymorphic pharmaceuticals and fine chemicals. *J Pharm Sci* 2005;94:1560–1576.
21. Gomes FP, Garcia PL, Alves JMP, Singh, AK, Kedor-Hackmann ERM, Santoro MIRM. Development and validation of stability-indicating HPLC methods for quantitative determination of pravastatin, fluvastatin, atorvastatin and rosuvastatin in pharmaceuticals. *Anal Lett* 2009;42:1784–1804.
22. Yu LX, Carlin AS, Amidon GL, Hussain AS. Feasibility studies of utilizing disk intrinsic dissolution rate to classify drugs. *Int J Pharm* 2004;270:221–227.
23. Yu LX, Amidon GL, Polli JE, Zhao H, Mehta MU, Conner DP et al. Biopharmaceuticals classification system: the scientific basis for biowaiver extensions. *Pharm Res* 2002;19:921–925.
24. Kasim NA, Whitehouse M, Ramachandran C, Bermejo M, Lennernäs H, Hussain AS et al. Molecular properties of WHO essential drugs and provisional biopharmaceutical classification. *Mol Pharm* 2004;1:85–96.
25. Moffat AC, Osselton MD, Widdop B. Clarke's analysis of drugs and poisons: in pharmaceuticals, body fluids and postmortem material. 3rd ed. London: Pharmaceutical Press, 2004.
26. Cermola F, Dellagrecia M, Iesce MR, Montanaro S, Previtera L, Temussi F, Brigante M. Irradiations of fluvastatin in water structure elucidation of photoproducts. *J Photochem Photobiol A* 2007;189:264–271.
27. Harris RK. NMR studies of organic polymorphs and solvates. *Analyst* 2006;131:351–373.
28. Carss, S, Harris RK, Fletton RA. Carbon-13 NMR investigations of three fluorinated steroids. *Magn Res Chem* 1995;33:501–505.
29. Park JS, Kang HW, Park SJ, Kim CK. Use of CP/MAS solid-state NMR for the characterization of solvate molecules within estradiol crystal forms. *Eur J Pharm Biopharm* 2005;60:407–412.
30. Bott RF, Oliveira WP. Storage conditions for stability testing of pharmaceuticals in hot and humid regions. *Drug Dev Ind Pharm* 2007;33:393–401.
31. Infantes L, Chisholm J, Motherwell S. Extended motifs from water and chemical functional groups in organic molecular crystals. *Cryst Eng Comm* 2003; 5:480–486.
32. Byrn SR, Pfeiffer RR, Stowell JG. Solid state chemistry of drugs. 2nd ed. Indiana: West Lafayette, 1999.
33. Budavari S. The Merck Index: an encyclopedia of chemicals, drugs and biologicals. 14th ed. New Jersey: Merck Research Laboratories, 2006: 143,722,968,1325,1471.

59
60
61
62
63
64
65
66
67
68
69
70
71
72
73
74
75
76
77
78
79
80
81
82
83
84
85
86
87
88
89
90
91
92
93
94
95
96
97
98
99
100
101
102
103
104
105
106
107
108
109
110
111
112
113
114
115
116